Scilight

Nonlinear Analysis and Computer Simulations
https://www.sciltp.com/journals/nacs

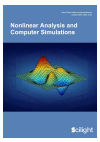

Article

Check for updates

Study of a Mixed Concave-Convex Sublinear-Superlinear Schrödinger System for Existence, Uniqueness, Classification and Computer Simulation

Anouar Ben Mabrouk [1,2,3]

[1] Department of Mathematics, Faculty of Science, University of Tabuk, King Faisal Road, Tabuk 47512, Saudi Arabia; anouar.benmabrouk@fsm.rnu.tn or amabrouk@ut.edu.sa
[2] Department of Mathematics, Higher Institute of Applied Mathematics and Computer Science, University of Kairouan, Street of Assad Ibn Alfourat, Kairouan 3100, Tunisia
[3] Laboratory of Algebra, Number Theory and Nonlinear Analysis, Faculty of Sciences, University of Monastir, Avenue of the Environnment, Monastir 5019, Tunisia

How To Cite: Ben Mabrouk, A. Study of a Mixed Concave-Convex Sublinear-Superlinear Schrödinger System for Existence, Uniqueness, Classification and Computer Simulation. *Nonlinear Analysis and Computer Simulations* **2026**, *1*(2), 7. https://doi.org/10.53941/nacs.2026.100007

Received: 19 November 2025
Revised: 2 February 2026
Accepted: 1 April 2026
Published: 15 April 2026

Abstract: In this paper, we are concerned with the study of a system of NLS equations in the presence of a superlinear convex and a sublinear concave nonlinearities correlating the couple of solutions such as $iu_t + \Delta u + |u|^{p-1}u + |v|^{q-1}u = 0$ and $iv_t + \Delta v + |v|^{p-1}v + |u|^{q-1}v = 0$. Existence, uniqueness and classification of the solutions are investigated provided with some numerical simulations via illustrating graphs. The simulations proved that possible chaotic behavior may be investigated. Moreover, the study allowed to emphasize the influence of the power law exponents and their strong impact on the initial conditions as well as the behavior of the solution.

Keywords: variational; energy functional; existence; uniqueness; NLS system; classification; simulation

2020 MSC: Primary: 35Q41; 35J50; Secondary: 35J10; 35Q55

1. Introduction

This present paper lies in the whole topic of nonlinear analysis of PDEs and their computer simulation. We precisely consider a couple of nonlinear Schrödinger equations linked with nonlinearities characterized by a correlation of superlinear and sublinear, convex and concave nonlinearities. Each nonlinear part constitutes a perturbation of the nonlinear system with the other one as a single nonlinearity. Combining two nonlinearities may be indeed regarded as a perturbation of the sub-linearity by means of a super-linearity to guarantee for example some regularity. In other words, each non-linearity guarantees some control to the other. We propose in the present work to develop results about existence, uniqueness, classification of solutions, and their behavior according to the parameters related to the problem. In addition, the possibility of the chaotic solutions or behavior is also investigated provided with computer simulations. Indeed, combining two nonlinearities in the present way may inform us about the effect of the superlinear perturbation on the solution of the sublinear problem and vice-versa. Does this perturbation permit to avoid strange behavior such that blow-up and chaotic?

Schrödinger equation since its discovery constitutes a challenging concept in physics as it models many phenomena in optics, plasma, fluid mechanics, etc. Enormous studies have investigated such an equation and the exact determination of solutions remains a complex task in the nonlinear case. In such a case, even if we know some solutions, the linear combination may not be a solution. Many types of solutions have been discovered in the nonlinear case such as solitons. Benci and Fortunato [1,2] developed variational methods for solitary waves, hylomorphic solitons and vortices, and for a system of solitary waves due to coupling the Maxwell equations with Klein-Gordon equation in a nonlinear case.

Recently, studies have been focused on the extension of such single equation to the case of a system of coupled equations of Schrödinger type and proved that such systems may describe better many phenomena in different fields such as simultaneous solitons, interaction of solitons, etc. Our paper is concerned with the investigation of the nonlinear system

$$\begin{cases} iu_t + u_{xx} + (|u|^{p-1} + |v|^{q-1})u = 0, \\ iv_t + v_{xx} + (|v|^{p-1} + |u|^{q-1})v = 0, \end{cases} \tag{1}$$

with suitable boundary conditions that will be fixed later. Here, $u = u(x,t)$ and $v = v(x,t)$ are complex-valued functions which may represent two simulatenous waves or moving particles, and are defined on $\mathbb{R} \times (t_0, +\infty)$, where $t_0 \in \mathbb{R}$ is an initial time. Furthermore, u_{xx} represents the second order partial derivative on x, and finally, u_t stands for the first order partial derivative on t.

Remark that for $u = v = \varphi$, we obtain the NLS form

$$i\varphi_t + \Delta\varphi + (|\varphi|^{p-1} + |\varphi|^{q-1})\varphi = 0, \tag{2}$$

which may itself lead to a system of coupled Heat equations by writing $\varphi = u + iv$, and thus getting

$$\begin{cases} u_t + \Delta v + \left((u^2+v^2)^{\frac{p-1}{2}} + (u^2+v^2)^{\frac{q-1}{2}}\right) v = 0, \\ v_t - \Delta u - \left((u^2+v^2)^{\frac{p-1}{2}} + (u^2+v^2)^{\frac{q-1}{2}}\right) u = 0. \end{cases} \tag{3}$$

Problem (2) was extensively examined, especially in [3–5] for numerical solutions in both 1-dimensional and higher dimensional cases. It is investigated for classification, nodal, non radial solutions, and phase plane analysis in [6–9]. A full study according to the power laws p, q was developed recently in [10]. Chaib [11] investigated a p-Laplacan system for necessary and sufficient conditions of existence. Hioe [12] considered the solitary wave solutions for a system of NLS equations involving power laws. Kanna et al. investigated in [13] the phenomenon of solitons collision in a mixed coupled NLS system. While Zhang et al. [14] investigated the phenomenon of bright solitons interactions for a two-dimensional coupled NLS system governing optical fibres. Zhida [15] showed the existence of multi-soliton solutions for a mixed NLS system in the presence of power laws.

Our principal goal is to consider the steady state solutions of problem (1) and study their behavior, existence, uniqueness and their classification relative to their initial values. To do this, denote

$$W(x,t) = (e^{i\omega t}u(x), e^{i\omega t}v(x)),$$

$\omega > 0$ a steady state solution. This makes problem (1) to be read as

$$\begin{cases} u_{xx} + (|u|^{p-1} + |v|^{q-1} - \omega)u = 0, \\ v_{xx} + (|v|^{p-1} + |u|^{q-1} - \omega)v = 0, \\ u(0) = a\,,\ v(0) = b\,,\ \ u'(0) = v'(0) = 0, \end{cases} \tag{4}$$

$a, b \in \mathbb{R}$ are the initial values. For the next parts of the paper, denote

$$g_\omega(x,y) = |x|^{p-1} + |y|^{q-1} - \omega \text{ and } f_\omega(x,y) = g_\omega(x,y)x, \quad (x,y) \in \mathbb{R}^2, \tag{5}$$

$$\Gamma_1 = \left\{(u,v) \in \mathbb{R}^2\,;\ |u|^{p-1} + |v|^{q-1} - \omega = 0\right\}, \tag{6}$$

$$\Gamma_2 = \left\{(u,v) \in \mathbb{R}^2\,;\ |v|^{p-1} + |u|^{q-1} - \omega = 0\right\}. \tag{7}$$

and

$$\Lambda = \left\{(u,v) \in \mathbb{R}^2\,;\ g_\omega(u,v) = g_\omega(v,u)\right\} \quad (= \{(u,v) \in \mathbb{R}^2;\ |u| = |v|\}). \tag{8}$$

Denote for the rest of the paper

$$\overline{\omega}_{pq} = \frac{p-1}{1-q},\ s_{pq} = \frac{q-1}{q-p},\ \text{ and } \omega_{pq} = \overline{\omega}_{pq}^{s_{pq}} + \overline{\omega}_{pq}^{s_{pq}-1}. \tag{9}$$

One fascinating motivation behind the present work is strongly related to the parameters p, q and ω. Indeed, the dependence of ω on ω_{pq} shows that a big difference may be noticed for the study of the problem. For $\omega < \omega_{pq}$, the curves Γ_1 and Γ_2 did not intersect, and they induce a partition of the whole plane $\mathbb{R}^2$ as shown in Figure 1. Here, all the partition elements are unbounded. Whenever $\omega = \omega_{pq}$, we get a unique intersection point of Γ_1 and Γ_2 in each quadrant of $\mathbb{R}^2$ ($\mathbb{R}^2_+$, $\mathbb{R}^2_-$, $\mathbb{R}_+ \times \mathbb{R}_-$, and $\mathbb{R}_- \times \mathbb{R}_+$) with a bounded cell at the origin. This is illustrated

by Figure 2. However, in the case where $\omega > \omega_{pq}$, we get two intersection points in each quadrant as shown in Figure 3. We will see that the boundedness or not of the partion cells has a strong link to the bahavior of the solution. Finally, we notice some symmetry of the partitions in all cases, which may be deduced from the problem itself. An extension to the case where each component has its proper frequency different from the other may be interesting. In such a case, we surely loss the symmetry of the problem.

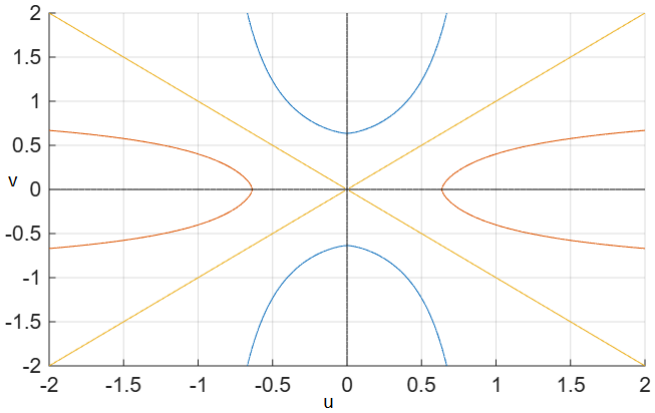

Figure 1. (Γ_1, Γ_2)-split of the space $\mathbb{R}^2$ for $p = 2.5$, $q = 0.5$ and $\omega = \omega_{pq} - 0.5$.

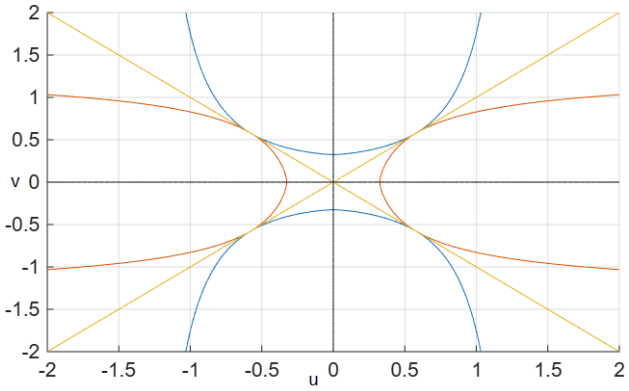

Figure 2. (Γ_1, Γ_2)-split of the space $\mathbb{R}^2$ for $p = 2.5$, $q = 0.5$ and $\omega = \omega_{pq}$.

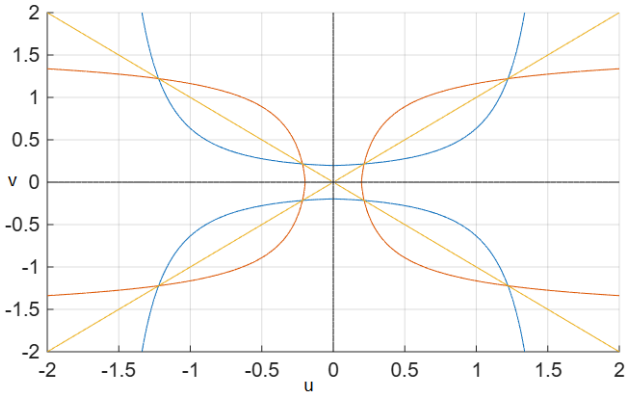

Figure 3. (Γ_1, Γ_2)-split of the space $\mathbb{R}^2$ for $p = 2.5$, $q = 0.5$ and $\omega = \omega_{pq} + 0.5$.

In the remaining parts of the present paper, we will consider this last case and thus assume that

$$0 < q < 1 < p \quad \text{and} \quad \omega > \omega_{pq}. \tag{10}$$

In [16–18], the mixed superlinear cubic case was investigated for $1 < p < 3$, $q = 3$ and $\omega > 1$. This may be easily obtained via our exact model (10). Indeed, by taking $q = 3$ as in [16–18], we get

$$\omega_{p3} = (-\overline{\omega}_{p3})^{s_{p3}} + (-\overline{\omega}_{p3})^{s_{p3}-1}, \tag{11}$$

which explains the comparison of the parameter p to 1 and 3, and next the interval of ω_{p3}. We may check for example that $\omega_{p3} \to 1$ as $p \to 3$. In the present paper we aim instead to study the sublinear case for the exponent q, and the superlinear case for the exponent p.

We now highlight the headlines of the paper. In Section 2, we develop our main results. In particular, we prove Theorems 1 and 2 about the existence of a unique solution to problem (4) and we investigate its behavior relative to the initial value in the representative cell $\Omega_1 \cup \Omega_2$. In the next section (Section 3), we consider the special case when the initial value lies on the frontiers of the cells Ω_i. This is special as on these frontiers, the model nonlinear functions are vanishing, and thus, the reasonning applied in the previous section may not be suitable. Concluding and future directions are next raised in Section 4.

2. Main Results

Recall firstly that some symmetries exists for the problem due to the parity of the nonlinear parts as well as the differential operators included in it. Therefore, we will consider, from now on, $(u(0), v(0)) = (a, b)$ in the first quadrant $\mathbb{R}^2_+$. The rest of cases may be deduced easily by symmetry. In this positive quadrant ($(a, b) \in \mathbb{R}^2_+$), there are four essential points to be used later; the origin $O(0, 0)$, $A(0, y_q)$, $B(z^1_{pq}, z^1_{pq})$, $C(x_p, 0)$ and $D(z^2_{pq}, z^2_{pq})$), where $x_p > 0$, and $y_q > 0$, are such that

$$x_p^{p-1} = y_q^{q-1} = \omega,$$

and $0 < z^1_{pq} < z^2_{pq}$ are the positive solutions of the equation

$$z^{p-1} + z^{q-1} = \omega.$$

In other words, we have $A = \Gamma_1 \cap (oy)$, $\{B, D\} = \Gamma_1 \cap \Gamma_2 \cap \Lambda$ and $C = \Gamma_2 \cap (ox)$, all in the positive quadrant $\mathbb{R}^2_+$. Figure 4 shows how the quadrant $\mathbb{R}^2_+$ is splitted due to Γ_1, Γ_2 and Λ. We get here a partition of the positive quadrant into eight cells. Due to the symmetry of the problem as well as the graphs, we will focus on the cells above the line $u = v$, which will be denoted as in Figure 4 by

$$\Omega_1 = \{(u, v) \in \mathbb{R}^2_+;\ 0 < u < v,\ f_\omega(u, v) < 0,\ f_\omega(v, u) > 0 \text{ and } g_\omega(u, v) < g_\omega(v, u)\},$$

$$\Omega_2 = \{(u, v) \in \mathbb{R}^2_+;\ u < v,\ f_\omega(u, v) > 0,\ f_\omega(v, u) > 0 \text{ and } g_\omega(u, v) < g_\omega(v, u)\},$$
$$\Omega_3 = \{(u, v) \in \mathbb{R}^2_+;\ u < v,\ f_\omega(u, v) < 0,\ f_\omega(v, u) < 0 \text{ and } g_\omega(u, v) < g_\omega(v, u)\},$$
$$\Omega_4 = \{(u, v) \in \mathbb{R}^2_+;\ u < v,\ f_\omega(u, v) > 0,\ f_\omega(v, u) > 0 \text{ and } g_\omega(u, v) < g_\omega(v, u)\}.$$

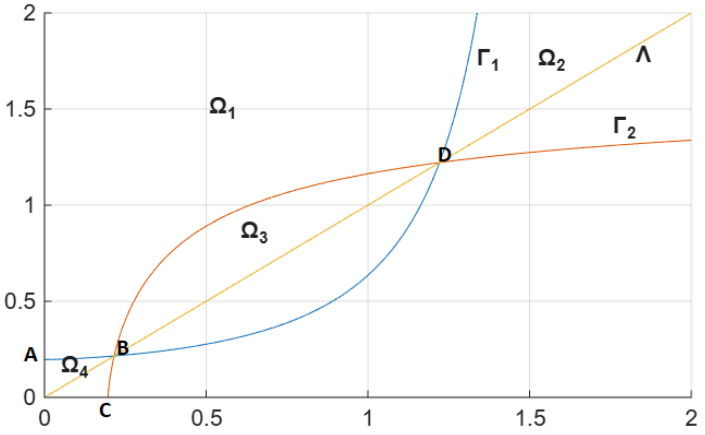

Figure 4. (Γ_1, Γ_2)-split of the quadrant $\mathbb{R}^2_+$ for $p = 2.5$, $q = 0.5$ and $\omega = \omega_{pq} + 0.5$.

Define for the sequel, the functional energy E

$$E(u, v)(x) = \frac{1}{2}(u_x^2 + v_x^2) + \frac{1}{p+1}(|u|^{p+1} + |v|^{p+1}) - \frac{\omega}{2}(u^2 + v^2) + F_q(u, v)(x), \tag{12}$$

where

$$F_q(u, v)(x) = \int_0^x (|u|^{q-1}vv' + |v|^{q-1}uu')dt.$$

Remark easily that E is constant as a function of x, and that

$$E(u,v)(x) = E(u,v)(0) = \frac{1}{p+1}(a^{p+1} + b^{p+1}) - \frac{\omega}{2}(a^2 + b^2),\ \forall\, x \in (0,\infty). \tag{13}$$

The following result concerns the case where the initial value is in Ω_1.

Theorem 1. *For $(u(0), v(0)) = (a, b) \in \Omega_1$, the problem (4) has a unique solution (u, v) satisfying*

i. *u and v are both oscillating,*
ii. *u and v are both infinitely sign-changing,*
iii. *(u, v) does not lie in any partition cell at infinity,*
iv. *u and v both have no limits at infinity.*

Proof. Existence and uniqueness of the solution is guarenteed via Appendix 4.

i. From the problem (4), we get at $x = 0$,

$$u''(0) = -f_\omega(a,b) > 0 \qquad \text{and} \qquad v''(0) = -f_\omega(b,a) < 0.$$

This means that u is non-decreasing and v is non-increasing on a small interval $(0, \delta)$. If we assume that both of them keep their same monotony on the whole domain $(0,\infty)$, then the limit $(l_u, l_v) = \lim\limits_{x\to\infty}(u(x), v(x))$ exists, and is finite due to the enrgy $E(u,v)(x)$. Due to the monotony of u, we see that $l_u > 0$. Assume that $l_v = 0$. So, the limit point will be equal to $C = (x_p, 0) = (l_u, 0)$. Hence, if $u(0) = a \geq x_p$, again the monotony of u leads to a contradiction as $x_p = l_u > u(0)$. Assume now that $a < x_p$. This means that to reach its limit the curve (u, v) must cross the curved path (A, B) in one point $M(u(x_1), v(x_1))$ and the segnment $[O, B]$ in one point $M(u(x_2), v(x_2))$. On the interval (x_2, ∞), we get from (4), u behaves as the solution $\widetilde{u}$ of the equation

$$\widetilde{u}'' + (p-1)\frac{w}{x_p}\widetilde{u} = 0,$$

which oscillates infinitely, and thus contradicts the brhavior of u being non-decreasing. So, $l_v \neq 0$. Therefore, we get necessarily $g_\omega(l_u, l_v) = g_\omega(l_v, l_u) = 0$, which means that $(l_u, l_v) = D$. In this case, we deduce that the fonction uv and $g_\omega(u,v) - g_\omega(v,u)$ keep a same sign, each one, on the whole interval $(0,\infty)$. So, multiplying the equations of (4) in order by v and u, and integrating the difference on $(0,\infty)$, we get

$$\int_0^\infty (g_\omega(u,v) - g_\omega(v,u))uvdx = 0,$$

which is impossible. We thus conclude that neither u nor v keeps its same monotony on $(0,\infty)$. Assume without loss of the generality that u remains non-decreasing and v non monotone. Assume that u increases to ∞ as x goes to ∞. By the first equation in the system (4), we deduce that

$$u(x) \leq u(R) + u'(R)(x-R) - \frac{1}{2}(x-R)^2,\ x \geq R,$$

for some $R > 0$ large enough. This is contradictory with u being increasing to ∞ as x goes to ∞. Assume now that u increases to a finite limit l_u as x goes to ∞, and v non monotone. Using the first equation in the system (4), we deduce that $|v|$ has a limit l_v satsifying $g_\omega(l_u, l_v) = 0$. We will show that $g_\omega(l_v, l_u) = 0$ also. If $g_\omega(l_v, l_u) = -\omega_0^2 < 0$, $\omega_0 \in \mathbb{R}_+$, the component v will behave at ∞ as $K_1\cos(\omega_0 x) + K_2\sin(\omega_0 x)$, ($K_1, K_2 \in \mathbb{R}$ constants), which has no limit as $x \to \infty$. If $g_\omega(l_v, l_u) = \omega_0^2 > 0$, $\omega_0 \in \mathbb{R}_+$, the component v will behave at ∞ as $K_1 e^{\omega_0 x} + K_2 e^{-\omega_0 x}$, ($K_1, K_2 \in \mathbb{R}$ constants), which is monotone as $x \to \infty$, which is again a contradiction (with v being non monotone). Consequently, we get the system $g_\omega(l_u, l_v) = g_\omega(l_v, l_u) = 0$ leading again to the limit $(l_u, l_v) \in \{B, D\}$. So, using similar techniques as above, we show that this is impossible. So as the item i is proved. Figure 5 illustrates the behavior of the solution (u, v) for $(u(0), v(0)) \in \Omega_1$ for x not large, and where we see easily the oscillating behavior.

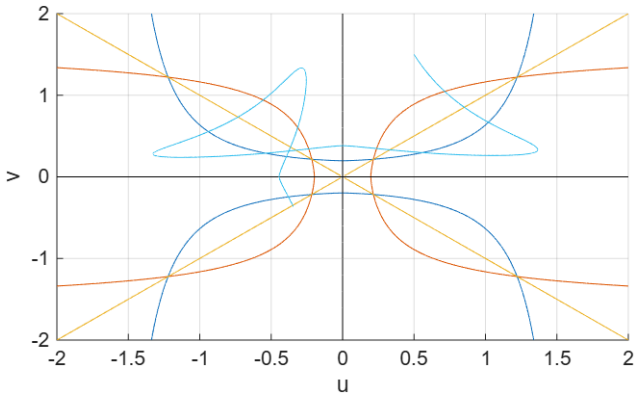

Figure 5. Simulation of (u, v) for $(u(0), v(0)) = (a, b) \in \Omega_1$, $p = 2.5$, $q = 0.5$, $\omega = \omega_{pq} + 0.5$, $a = 0.5$ and $b = 1.5$.

ii. Figure 6 illustrates the behavior of the solution (u, v) for an initial value $(u(0), v(0)) = (a, b) \in \Omega_1$, where we see easily that the sign-changing appears more and more as x grows up. Moreover, the solution (u, v) does not lie in any cell, which will be subject of item iii.

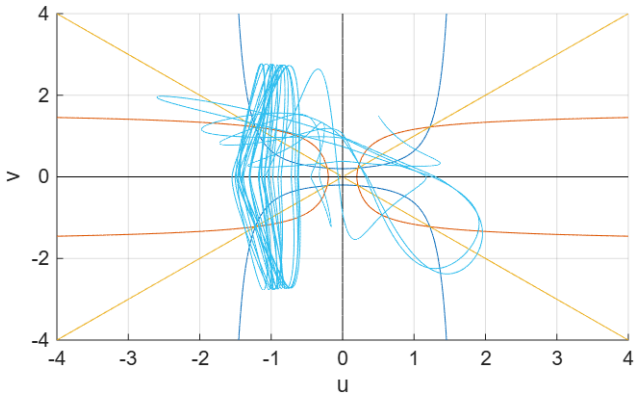

Figure 6. Simulation of (u, v) for $(u(0), v(0)) = (a, b) \in \Omega_1$, $p = 2.5$, $q = 0.5$, $\omega = \omega_{pq} + 0.5$, $a = 0.5$ and $b = 1.5$, x being large.

Let us prove the result theoretically. Assume that the contrary holds, and that u remains positive at ∞. Denote

$$h_\infty = \int_R^\infty f_0(t) e^{\sqrt{\omega} t} dt,$$

($f_0 = -f_\omega$, for $\omega = 0$). It follows that at ∞, the component u behaves as the solution $\widetilde{u}$ of the equation

$$\widetilde{u}'' - \omega \widetilde{u} = f_0(x), \ x \in (R, \infty),$$

with some $R > 0$ large enough. However, remark that $\widetilde{u}$ itself behaves at ∞ as $h_\infty e^{\sqrt{\omega} x}$, which contradicts the positivity of u at ∞.

iii. Assume that the contrary holds, and that (u, v) lies in one cell, for example in $\overline{\Omega_1}$ at infinity. This yields that both u and v keep (each one) a same sign at infinity, which contradicts item ii.

iv. This item is a natural deduction from previous ones. □

Figure 7 illustrates the behavior of the pair solution (u, v) for $(u(0), v(0)) = (a, b) \in \Omega_1$, where we see easily that it is infinitely sign-changing and does not lie in any cell as x goes to ∞.

Remark 1. *The oscillatory behavior in Theorem 1 item i (and other contexts in the paper) is considered in the sense that for any real number R, the function is not monotone on (R, ∞).*

The results of Theorem 1 may be extended to all the interiors of the remaining partition cells. Recall that the curves Γ_1, Γ_2 and Λ split the plan $\mathbb{R}^2$ into 32 cells. Due to the symmetry in the problem, the cells Ω_1, Ω_2, Ω_3 and Ω_4 yield the remaining cells by means of the symmetries S_x (due to the x-axis), S_y (due to the y-axis),

$S_{x=y}$ (due to the line $x = y$), $S_{x=-y}$ (due to the line $x = -y$), and finally S_O (due to the origin O). We thus get the following second main result.

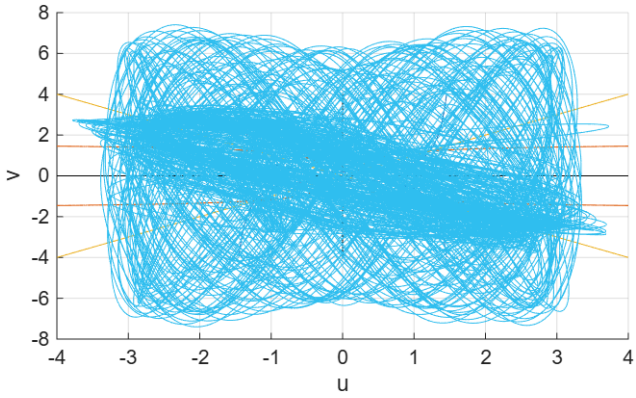

Figure 7. Simulation of (u, v) for $(u(0), v(0)) = (a, b) \in \Omega_1$, $p = 2.5$, $q = 0.5$, $\omega = \omega_{pq} + 0.5$, $a = 0.5$ and $b = 1.5$, x being large enough.

Theorem 2. *Assume that* $(u(0), v(0)) = (a, b)$ *belongs to the interior of any partition cell, the problem (4) has a unique solution* (u, v) *for which* u *and* v *are both oscillating, infinitely sign-changing, and both have no limits at infinity. Moreover,* (u, v) *does not lie in any partition cell at infinity.*

Figures 8 and 9 illustrate some cases of the phase plane portraits (u', u) and (v', v), respectively, for the solution (u, v). The figures confirm the oscillating behavior raised in Theorem 1. For these figures, the parameters of the problem are fixed to $p = 2.5$, $q = 0.5$, and $\omega = \omega_{pq} + 0.5 = 2.25$.

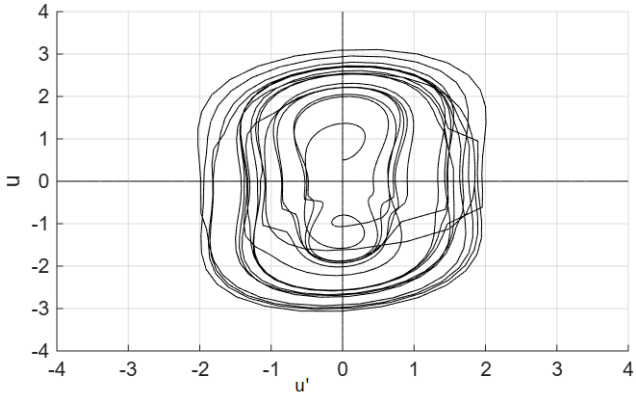

Figure 8. Simulated phase plane (u', u) with $(a, b) = (0.5, 1.5) \in \Omega_1$, $p = 2.5$, $q = 0.5$, and $\omega = 2.25$.

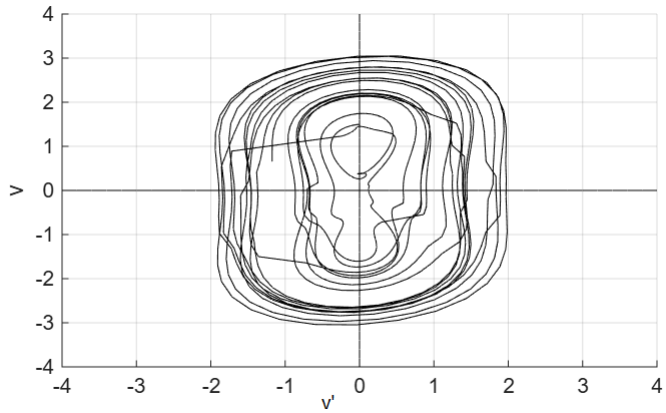

Figure 9. Simulated phase plane (v', v) with $(a, b) = (0.5, 1.5) \in \Omega_1$, $p = 2.5$, $q = 0.5$, and $\omega = 2.25$.

Now, as for the previous cases, we plot in Figures 10–12 some graphic simulations of the behavior of the solution as well as the phase plane portraits for one of the other partition cells, such as the cell Ω_2.

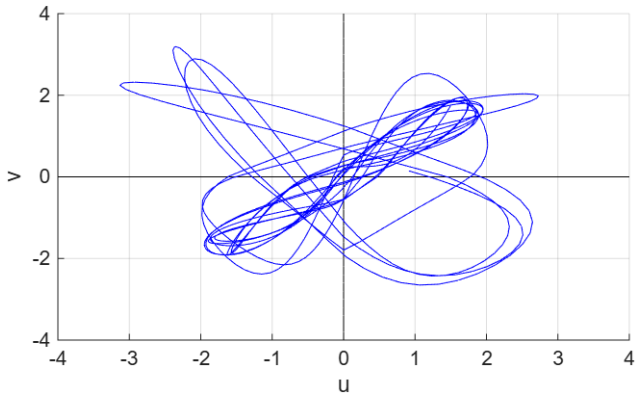

Figure 10. The solution (u, v) with $(a, b) = (1.5, 1.75) \in \Omega_2$, $p = 2.5$, $q = 0.5$, and $\omega = 2.25$.

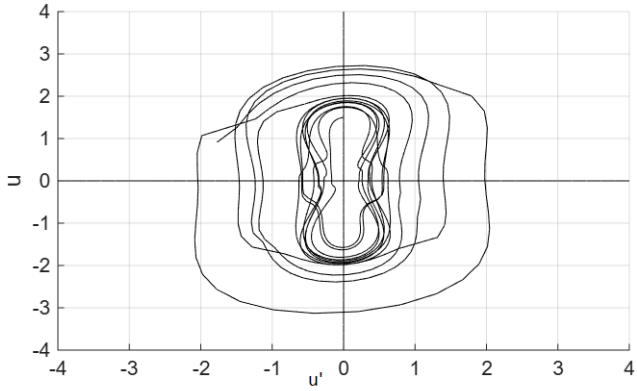

Figure 11. The portrait (u', u) with $(a, b) = (1.5, 1.75) \in \Omega_2$, $p = 2.5$, $q = 0.5$, and $\omega = 2.25$.

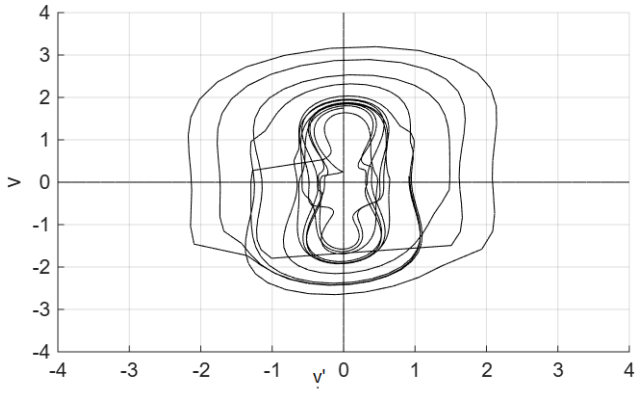

Figure 12. The portrait (v', v) with $(a, b) = (1.5, 1.75) \in \Omega_2$, $p = 2.5$, $q = 0.5$, and $\omega = 2.25$.

3. Study of the Essential Special Cases

In this section, we examine the problem (4) when the initial value (a, b) lies on the frontiers of the different partition cells. Some cases are natural such as when $(u, v)(0) = (a, b) \in \{O, B, D\}$ and their symmetric points according to the symmetries of the problem mentioned previously. In these cases, we get the constant solutions.

3.1. Case 1: $(a, b) = (0, y_q) = A$

In this section, we get immediately $u \equiv 0$, and our system will be reduced to

$$\begin{cases} v'' + (|v|^{p-1} - w)v = 0 & , \quad x \in (0, \infty), \\ v(0) = b = y_q & , \quad v'(0) = 0, \end{cases} \tag{14}$$

where we recall that $y_q = w^{\frac{1}{1-q}} > 1$. Denote next

$$g_\omega(v) = |v|^{p-1} - w, \quad f_\omega(v) = g_\omega(v)v \quad \text{and} \quad F_\omega(v) = \frac{1}{p+1}|v|^{p+1} - \frac{w}{2}v^2.$$

The functions g_ω and f_ω have the same positive zero x_p. Denote thus z_1 and z_2 the respective positive zeros of the functions f'_ω and F_ω,

$$z_1 = (\frac{w}{p})^{1/p-1} \quad \text{and} \quad z_2 = (\frac{w(p+1)}{2})^{1/p-1}, \tag{15}$$

Consider as usual the functional energy (for problem (14)),

$$E(v)(x) = \frac{1}{2}v'(x)^2 + \frac{1}{p+1}|v|^{p+1} - \frac{w}{2}v^2 = \frac{1}{2}v'(x)^2 + F_\omega(v).$$

Remark, as in the previous cases, that $E(v)$ is constant, and

$$E(v)(x) = E(v)(0) = \frac{1}{p+1}y_q^{p+1} - \frac{w}{2}y_q^2 = F_\omega(y_q).$$

This yields that the solution v is bounded, and more precisely, $-y_q \leq v \leq y_q$ on $(0,\infty)$. Notice next that, at the origin, we have $v''(0) = -(y_q^{p-1} - w)y_q < 0$. This implies that the function v is nonincreasing on $(0,\delta)$ for $\delta > 0$ small enough. If it remains monotone on $(0,\infty)$, it has a finite limit l. If $l = 0$, then the solution v will behave as $K_1 e^{-\sqrt{w}x} + K_2 e^{\sqrt{w}x}$, which contradicts the property of being bounded, and its energy being constant. So, it remains that $l^{p-1} = w$, or equivalently, $l = x_p$. This reads that v behaves (at ∞) as the function $\widetilde{v}$ solution of

$$\widetilde{v}" + w(p-1)(\widetilde{v} - x_p) = 0.$$

As $p > 1$, $\widetilde{v}$ is oscillatory, and so as v, which is contradictory. Hence, v is oscillatory on $(0,\infty)$ infinitely. Denote $\zeta_0 < \zeta_1 < \zeta_2 < \cdots < \zeta_{2k} < \zeta_{2k+1} \ldots$, $k \in \mathbb{N}$ its critical points such that ζ_{2k}, $k \in \mathbb{N}$ are maxima and ζ_{2k+1}, $k \in \mathbb{N}$ are minima. It holds that

$$v(\zeta_{2k}) < x_p < v(\zeta_{2k+1}),\ \forall k \geq 0.. \tag{16}$$

Indeed, for $k = 0$, we have $v(\zeta_0) = v(0) = y_q < x_p$. Whenever $v(\zeta_1) < x_p$, we get from (14),

$$0 = \int_{\zeta_0}^{\zeta_1} v"dx = -\int_{\zeta_0}^{\zeta_1} f_\omega(v)dx > 0,$$

which is not possible. The rest follows by induction on k. Remark here that the solution v remains positive on the whole interval $(0,\infty)$. This may be proved by using classical techniques such as [6,10].
By the symmetry, we get solutions oscillating around $-x_p$. We obtain the following result.

Theorem 3. *Problem (14) possesses a unique solution v, which is positive and oscillating around x_p infinitely. Moreover, there exists sequences $(\xi_k)_k$ and $(\zeta_k)_k$ for which $v(\xi_k) = x_p$, $v'(\zeta_k) = 0$, $\forall k \geq 0$, and*

$$0 = \zeta_0 < \xi_1 < \zeta_1 < \xi_2 < \ldots < \zeta_{2k} < \xi_{2k+1} < \zeta_{2k+1} < \xi_{2k+2} < \ldots \uparrow +\infty. \tag{17}$$

Moreover, (v', v) lies on the ellipsoidal-type curve

$$\mathcal{E}_{w,p,b} = \left\{(x,y) \in \mathbb{R}^2;\ (p+1)x^2 + 2|y|^{p+1} - w(p+1)y^2 = 2y_q^{p+1} - w(p+1)y_q^2\right\}. \tag{18}$$

Figures 13 and 14 illustrate the results of this case graphically. In Figure 13, we notice easily the oscillating behavior (infinitely), the positivity of v, and on Figure 14, it is noticeable that the ellipsoidal-type curve $\mathcal{E}_{w,p,b}$ encloses the couple (v', v) on the whole interval $(0,\infty)$.

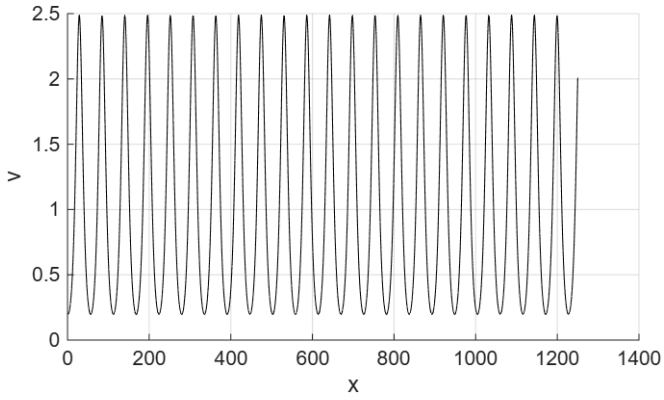

Figure 13. The solution v of problem (14), $p = 2.5$, $q = 0.5$, and $\omega = 2.25$.

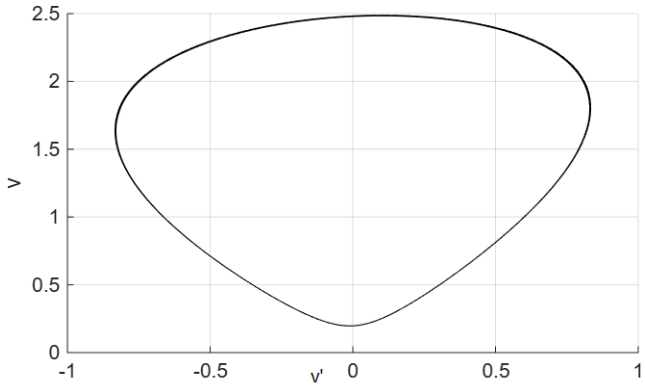

Figure 14. The portrait (v', v) of problem (14), $p = 2.5$, $q = 0.5$, and $\omega = 2.25$.

3.2. Case 2: $(a, b) \in (O, A)$

In this case $(u(0), v(0)) = (0, b)$, with $b \in (0, y_q)$. On $(0, \delta)$, $\delta > 0$, (small enough), our system (4) will behave as the system

$$\begin{cases} u'' + (b^{q-1} - w)u = 0 & , \quad x \in (0, \infty), \\ v'' + (b^{p-1} - w)v = 0 & , \quad x \in (0, \infty), \\ u(0) = 0,\ v(0) = b \in (0, y_q) & , \quad u'(0) = v'(0) = 0. \end{cases} \tag{19}$$

We will show here that $u \equiv 0$. Indeed, the first equation in system (19) leads to

$$u(x) = C_1 \cos(w_0 x) + C_2 \sin(w_0 x),\ x \in (0, \delta),$$

$w_0^2 = b^{q-1} - w$, and C_1, C_2 being constants. So, by exploiting the initial data $u(0) = u'(0) = 0$, we get $C_1 = C_2 = 0$. Hence, $u \equiv 0$ on $(0, \delta)$. So, it is vanishing on the whole interval $(0, \infty)$. The system (4) reduces to

$$\begin{cases} v'' + (|v|^{p-1} - w)v = 0 & , \quad x \in (0, \infty), \\ v(0) = b \in (0, y_q) & , \quad v'(0) = 0. \end{cases} \tag{20}$$

We therefore obtain an analog result to the previous case resumed in the following theorem.

Theorem 4. *Problem (20) possesses a unique solution v which is positive and oscillating around x_p infinitely without limit at infinity. Moreover, there exists sequences $(\xi_k)_k$ and $(\zeta_k)_k$ for which $v(\xi_k) = x_p$, $v'(\zeta_k) = 0$, $\forall k \geq 0$, and (17). Furthermore, the portrait (v', v) lies on the ellipsoidal-type curve*

$$\mathcal{E}_{w,p,b} = \left\{(x, y) \in \mathbb{R}^2;\ (p+1)x^2 + 2|y|^{p+1} - w(p+1)y^2 = 2b^{p+1} - w(p+1)b^2\right\}. \tag{21}$$

3.3. Case 3: $(a, b) \in (A, i\infty) = \{0\} \times (y_q, \infty)$

In this case also, we get a null solution u, and a reduced system

$$\begin{cases} v'' + (|v|^{p-1} - w)v = 0 & , \quad x \in (0, \infty), \\ v(0) = b \in (y_q, \infty) & , \quad v'(0) = 0. \end{cases} \tag{22}$$

In this case, we have the following theorem.

Theorem 5. *Problem (22) admits a unique solution v, which is oscillating around x_p infinitely being positive, or oscillating around 0 infinitely, without limit at infinity in both cases. Moreover, there exists sequences $(\xi_k)_k$ and $(\zeta_k)_k$ such that $v(\xi_k) = x_p$ or 0, $v'(\zeta_k) = 0$, $\forall k \geq 0$, and (17). Besides, the portrait (v', v) lies on the ellipsoidal-type curve $\mathcal{E}_{w,p,b}$ in (21).*

Figure 15 shows the oscillating behavior of the solution v around x_p and its positivity on the whole interval $(0, \infty)$, for an initial value $v(0) \in (y_q, z_2)$. Recall that z_2 is defined in (15). Figure 16 shows a similar behavior of v for $v(0) = z_2$. Figure 17 is obtained for an initial value $v(0) > z_2$. It shows the oscillating behavior of the solution v around 0, and thus it is sign-changing infinitely.

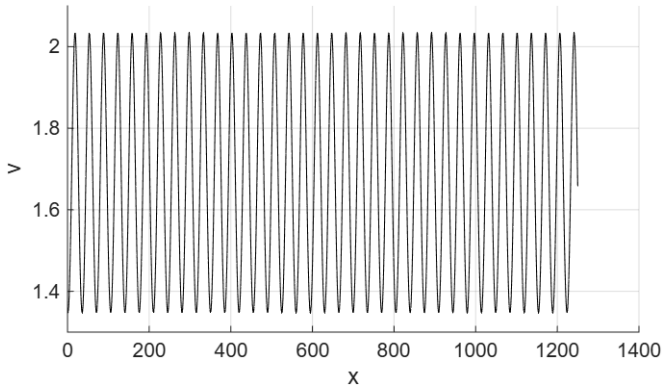

Figure 15. A simulation of v solution to problem (22) for $y_q < b < z_2$, $p = 2.5$, $q = 0.5$, and $\omega = 2.25$.

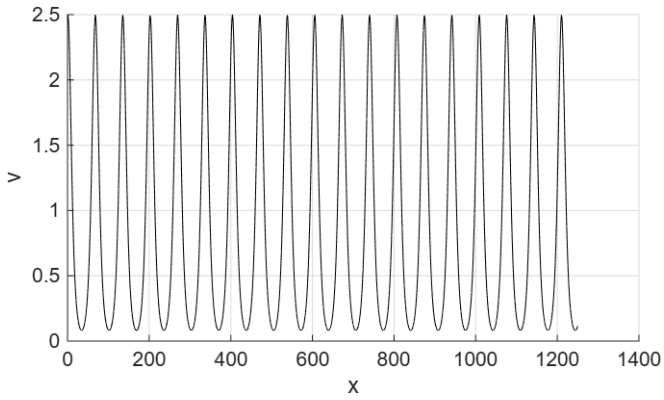

Figure 16. A simulation of v solution to problem (22) for $b = z_2$, $p = 2.5$, $q = 0.5$, and $\omega = 2.25$.

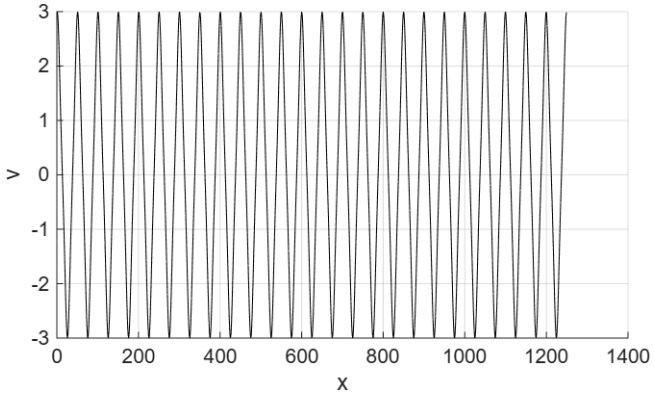

Figure 17. A simulation of v solution to problem (22) for $b = z_2 + 0.5$, $p = 2.5$, $q = 0.5$, and $\omega = 2.25$.

3.4. Case 4: $(a,b) \in (A,B)$

In this case, the solutions u and v start nondecreasing on $(0,\delta)$, $\delta > 0$ (small enough). If they keep the same monotony on the whole interval $(0,\infty)$, we get respective limits l_u and l_v. Such limits are positive and finite due to the monotony of u and v, and the energy $E(u,v)$ of the system. As a result, $(l_u,l_v) \in \{B,D\}$. Whenever $(l_u,l_v) = B$, the system (4) behaves at infinity as the system

$$\begin{cases} u'' + (p-1)(z^1_{pq})^{p-1}u + (q-1)(z^1_{pq})^{q-1}v = 0, \\ v'' + (q-1)(z^1_{pq})^{q-1}u + (p-1)(z^1_{pq})^{p-1}v = 0. \end{cases} \tag{23}$$

For simplicity, write $\alpha = (p-1)(z^1_{pq})^{p-1}$ and $\beta = (q-1)(z^1_{pq})^{q-1}$, and denote

$$X = \begin{pmatrix} u \\ u' \\ v \\ v' \end{pmatrix} \quad \text{and} \quad M = \begin{pmatrix} 0 & 1 & 0 & 0 \\ -\alpha & 0 & -\beta & 0 \\ 0 & 0 & 0 & 1 \\ -\beta & 0 & -\alpha & 0 \end{pmatrix}.$$

The system (23) above is equivalent to the dynamical system

$$X' = MX.$$

Standard computations yield that the characteristic equation of this last system is

$$(r^2+\alpha)^2 + \beta^2 = 0,$$

which has four different complex roots $\gamma = \gamma_0 + i\gamma_1$, its complex conjugate $\overline{\gamma}$, $-\gamma$ and $-\overline{\gamma}$, with $\gamma_1 \neq 0$. This leads to an oscillatory solution (u,v), which contradicts the monotony. The same techniques hold for the case $(l_u,l_v) = D$. We conclude that the solutions u and v are not monotone, and are instead oscillating infinitely as follows.

Theorem 6. *For $(u(0),v(0)) = (a,b) \in (A,B)$, problem (4) possesses a unique solution (u,v) for which u and v are oscillating infinitely around 0 and x_p, respectively, without limits at infinity. Moreover, v is positive.*

Figure 18 shows the bahavior of the solution (u,v) near 0. It shows clearly the monotony near 0, and that the solution crosses the cell $\overline{\Omega_1}$. A first turning point where $v' = 0$ is obtained in Ω_1. Figure 19 illustrates the behavior of the solution for x being more large. It crosses the quadrant $x,y > 0$ to the opposite one $x < 0,\ y > 0$, which confirms effectively that the component u is sign-changing and v keeps a positive sign. Figure 20 shows the behavior of the solution (u,v) for x being large enough, where we notice easily a confirmation of Theorem 6 results. Figures 21 and 22 show the behavior of the components u and v separately for more clarity. u oscillates infinitely around 0, and v oscillates infinitely around x_p. The component v keeps a positive sign.

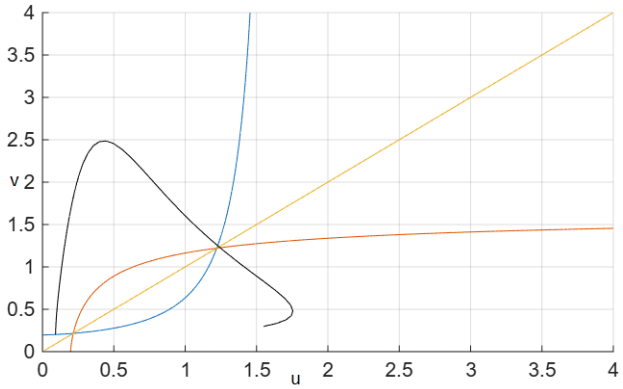

Figure 18. Simulation of (u,v) near 0 for $(a,b) \in (A,B)$, $p = 2.5$, $q = 0.5$, and $\omega = 2.25$.

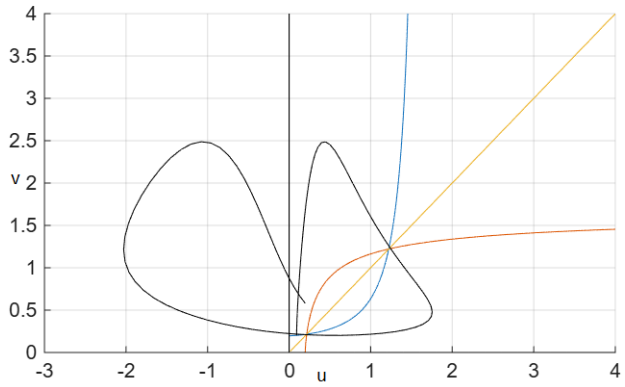

Figure 19. Simulation of (u, v) for larger values of x for $(a, b) \in (A, B)$, $p = 2.5$, $q = 0.5$, and $\omega = 2.25$.

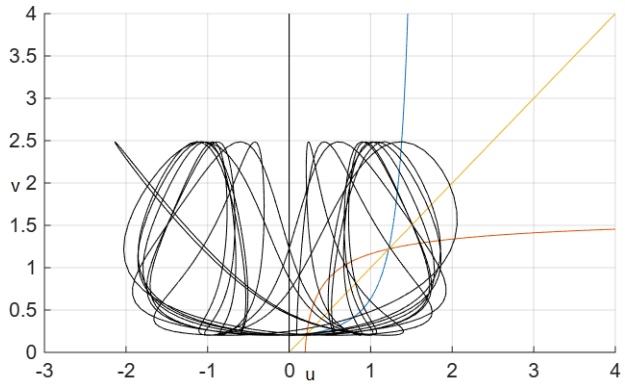

Figure 20. Simulation of (u, v) on a highly large interval for $(a, b) \in (A, B)$, $p = 2.5$, $q = 0.5$, and $\omega = 2.25$.

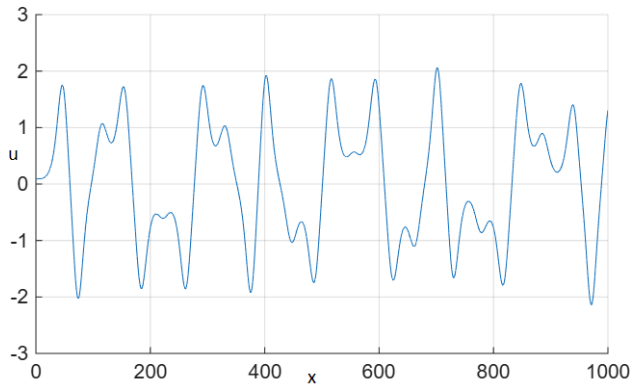

Figure 21. Simulated solution u for $(a, b) \in (A, B)$, $p = 2.5$, $q = 0.5$, and $\omega = 2.25$.

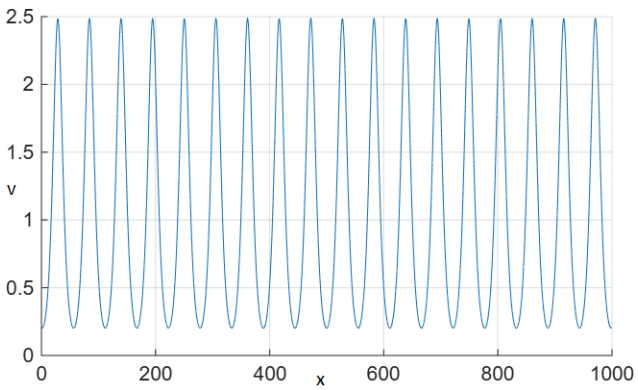

Figure 22. Simulated solution v for $(a, b) \in (A, B)$, $p = 2.5$, $q = 0.5$, and $\omega = 2.25$.

3.5. Case 5: $(a,b) \in (B,D)$ *on* Γ_1

Theorem 7. *For* $(u(0),v(0)) = (a,b) \in (B,D)$*, problem (4) admits a unique solution* (u,v) *such that*

i. u *is oscillating around* 0 *infinitely,*
ii. v *is positive oscillating around* x_p *infinitely,*
iii. both u *and* v *have no limits at infinity.*

This case resembles to the previous one. They just differ in the positions of the critical points of the solutions. Figure 23 shows the bahavior of the solution (u,v) near 0. A first turning point where $v' = 0$ is out of the cell Ω_1. Figure 24 illustrates the behavior of the solution for x being more large. It also crosses the quadrant $\mathbb{R}_+^2$ to the opposite one $\mathbb{R}_- \times \mathbb{R}_+$. Figure 25 shows a simulation of (u,v) for x being large enough.

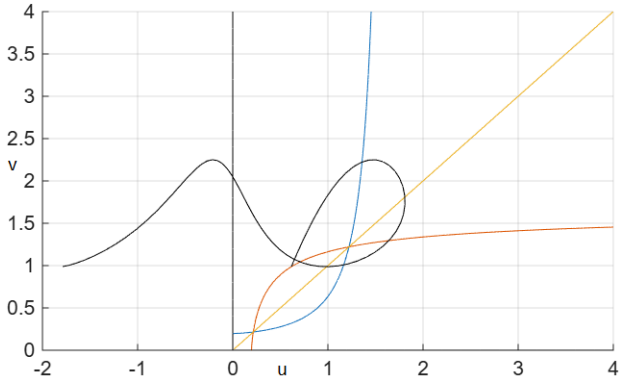

Figure 23. Simulation of (u,v) near 0 for $(a,b) \in (B,D)$, $p = 2.5$, $q = 0.5$, and $\omega = 2.25$.

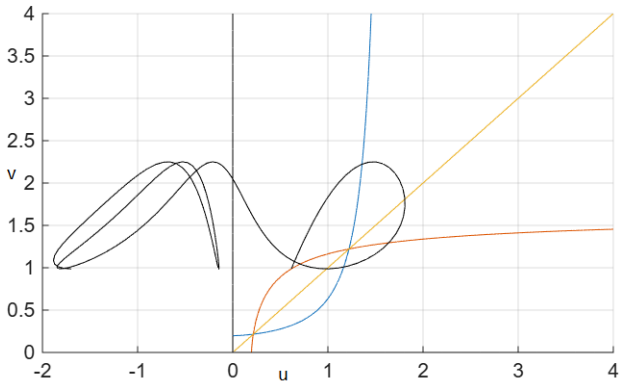

Figure 24. Simulation of (u,v) for larger values of x for $(a,b) \in (B,D)$, $p = 2.5$, $q = 0.5$, and $\omega = 2.25$.

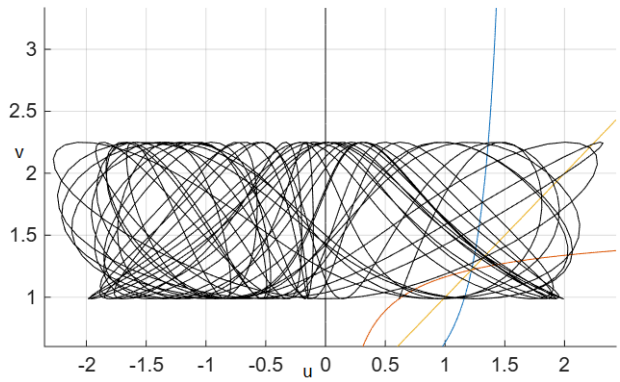

Figure 25. Simulation of (u,v) on a highly large interval for $(a,b) \in (B,D)$, $p = 2.5$, $q = 0.5$, and $\omega = 2.25$.

3.6. Case 6: $(a,b) \in (D,\infty)$ *on* Γ_2

Theorem 8. *For* $(u(0),v(0)) = (a,b) \in (D,\infty)$ *on* Γ_2*, problem (4) admits a unique solution* (u,v) *for which*

i. u *and* v *are oscillating infinitely without limits at infinity,*
ii. u *and* v *are both infinitely sign-changing,*
iii. (u, v) *does not lie in any partition cell.*

Figure 26 shows the bahavior of the solution (u, v) near 0. It shows clearly the monotony near 0, and that the solution crosses quitely all the cells. A first turning point where $v' = 0$ is obtained in the symmetric cell to Ω_1 according to the x-axis. Figure 27 illustrates a more complex behavior of the solution for x being more large. It continues to cross all the cells or the quadrants of the plan $\mathbb{R}^2$. Figure 28 shows a simulation of the solution (u, v) for x being large enough, where we notice easily a confirmation of Theorem 8 results. Figures 29 and 30 show the behavior of the components u and v separately for more clarity. Both u and v oscillate infinitely with sign-changing and no previledged limits.

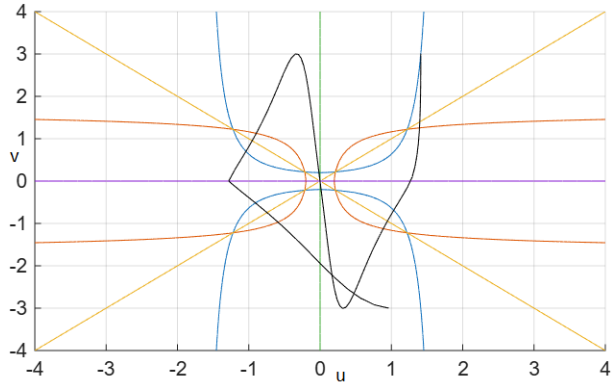

Figure 26. Simulation of (u, v) near 0 for $(a, b) \in (D, \infty)$ on Γ_2, $p = 2.5$, $q = 0.5$, and $\omega = 2.25$.

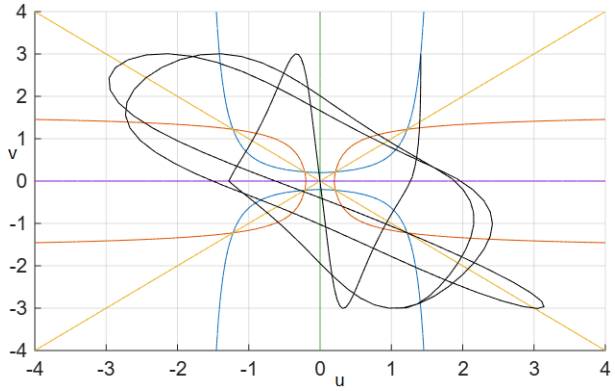

Figure 27. Simulation of (u, v) for larger values of x for $(a, b) \in (D, \infty)$ on Γ_2, $p = 2.5$, $q = 0.5$, and $\omega = 2.25$.

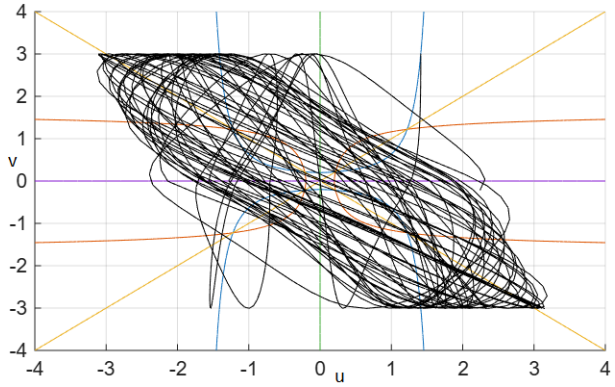

Figure 28. Simulation of (u, v) on a highly large interval for $(a, b) \in (D, \infty)$ on Γ_2, $p = 2.5$, $q = 0.5$, and $\omega = 2.25$.

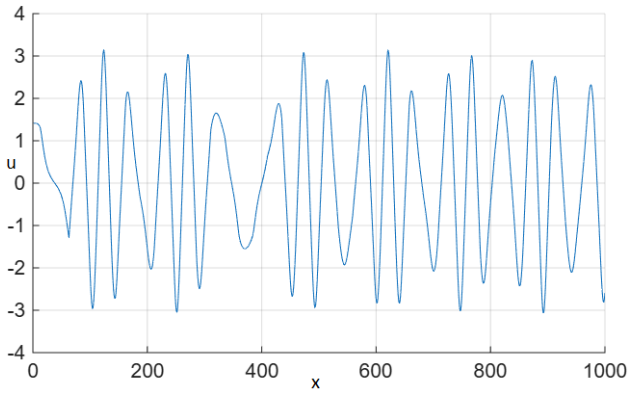

Figure 29. Simulation of u on a highly large interval for $(a, b) \in (D, \infty)$ on Γ_2, $p = 2.5$, $q = 0.5$, and $\omega = 2.25$.

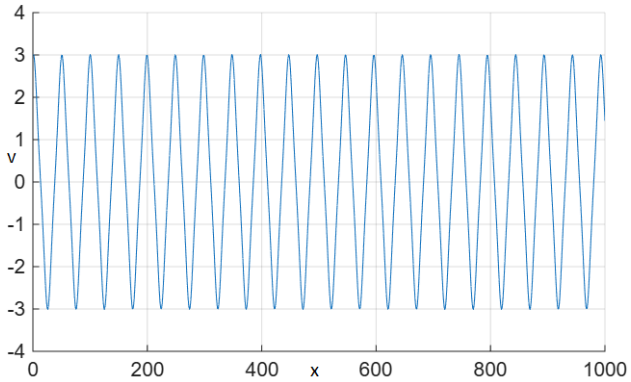

Figure 30. Simulation of v on a highly large interval for $(a, b) \in (D, \infty)$ on Γ_2, $p = 2.5$, $q = 0.5$, and $\omega = 2.25$.

3.7. Case 7: $(a, b) \in (D, \infty)$ *on* Λ

Theorem 9. *For* $(u(0), v(0)) = (a, b) \in (D, \infty)$ *on* Γ_2, *problem (4) possesses a unique solution* (u, v) *such that*

i. u *and* v *are oscillating,*
ii. u *and* v *are positive,*
iii. $(u, v) \in \overline{\Omega_1 \cup \Omega_2}$.

Figure 31 shows the bahavior of the solution (u, v) near 0 showing the monotony near 0, the crossing of the cell $\overline{\Omega_2}$ to Ω_1. A first turning point where $v' = 0$ is obtained in Ω_1. Figure 32 illustrates the behavior of the solution for x being more large. It lies in the positive quadrant $x, y > 0$ confirming effectively that the component u and v are both positive. Figure 33 shows fascinately a simulation of (u, v) for x being large enough, where we notice easily a confirmation of Theorem 9 results.

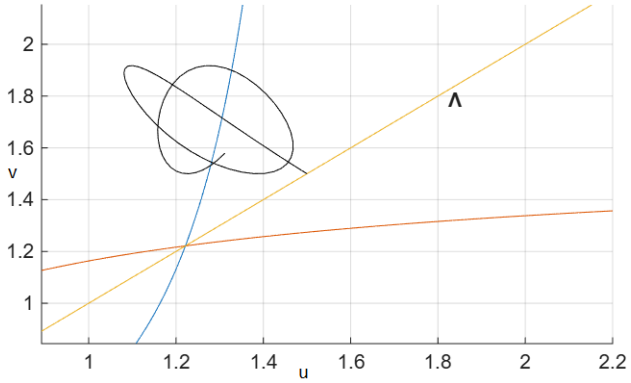

Figure 31. Simulation of (u, v) near 0 for $(a, b) \in (D, \infty)$ on Λ, $p = 2.5$, $q = 0.5$, and $\omega = 2.25$.

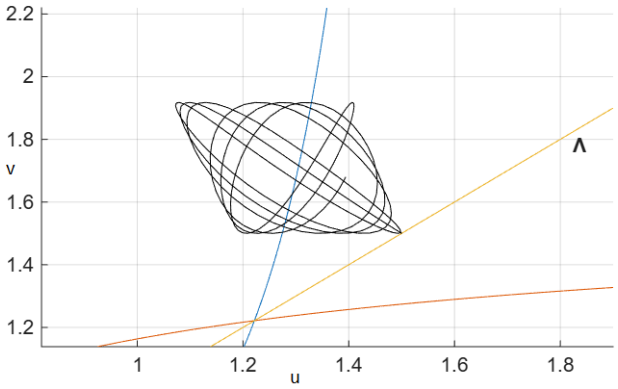

Figure 32. Simulation of (u, v) for larger values of x for $(a, b) \in (D, \infty)$ on Λ, $p = 2.5$, $q = 0.5$, and $\omega = 2.25$.

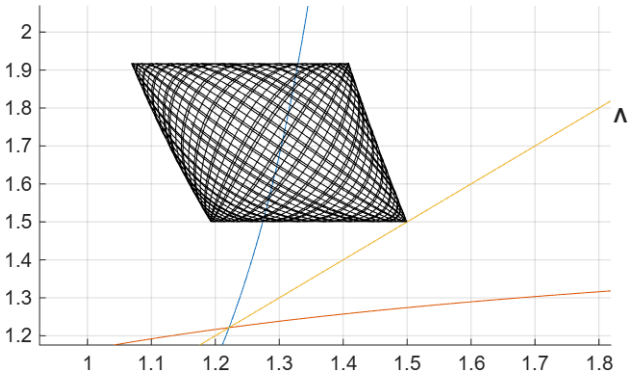

Figure 33. Simulation of (u, v) on a highly large interval for $(a, b) \in (D, \infty)$ on Λ, $p = 2.5$, $q = 0.5$, and $\omega = 2.25$.

4. Conclusions

In the present paper, a coupled NLS system is examined in the presence of mixed nonlinearities. One nonlinear part is odd, superlinear and convex, and a second is odd, sublinear and concave, aasuring some correlation between the pair of solutions. The problem is considered for the existence, uniqueness and classification of the steady state solutions according to the power law parameters, the pulsation and the initial data. Numerical simulations are also provided to illustrate graphically the behavior of the solutions such as oscillating and phase plane portraits. The present work joins a series of works on coupled NLS systems such as [2, 16–24] and opens the path to investigate other cases relative to the problem parameters and eventual dynamical systems issued from it like chaotic behavior.

Institutional Review Board Statement

Not applicable.

Informed Consent Statement

Not applicable.

Data Availability

Not applicable.

Acknowledgments

The author would like to thank the editor and the anonymous reviewers for the interest given to the work. Their comments and suggestions improved the paper well.

Conflict of interest

The author declares no conflict of interest.

Use of AI and AI-Assisted Technologies

No AI tools were utilized for this paper.

Appendix A. On the Existence and Uniqueness of the Solution

In this appendix, we recall briefly the idea that guarantee the existence and uniqueness of the solution of the NLS systems investigated. In fact many cases may be treated via the well-known Cauchy-Lipschitz theory and also by using iterative methods applied to suitable integral equations. We will adopt here an approach based on fixed point theory. We will recall the first case on the cell Ω_1. The other cases may be treated by similar ideas with suitable and/or necessary modifications.

Let $(u(0), v(0)) = (a, b) \in \Omega_1$, and consider the set

$$M_{a,b} = \{(u, v) \in \mathcal{C}((0, \delta)); \;\; a \leq u(x) \leq ca, \;\; c^{-1}b \leq v(x) \leq b, \;\; x \in (0, \delta)\},$$

for $\delta > 0$ small enough and $c > 1$ fixed. From the system (4), we get

$$\begin{cases} u(x) = a - x^2 \displaystyle\int_0^1 \int_0^1 \theta f_\omega(u, v)(x\theta\eta) d\eta d\theta, \\ \\ v(x) = b - x^2 \displaystyle\int_0^1 \int_0^1 \theta f_\omega(v, u)(x\theta\eta) d\eta d\theta, \end{cases} \quad x \in (0, \delta). \tag{A1}$$

Denote next $\Phi : M_{a,b} \to M_{a,b} \cap \mathcal{C}^2$ defined by

$$\Phi(u, v) = (\Phi_1(u, v), \Phi_2(u, v)),$$

with

$$\begin{cases} \Phi_1(u, v)(x) = a - x^2 \displaystyle\int_0^1 \int_0^1 \theta f_\omega(u, v)(x\theta\eta) d\eta d\theta, \\ \\ \Phi_2(u, v)(x) = b - x^2 \displaystyle\int_0^1 \int_0^1 \theta f_\omega(v, u)(x\theta\eta) d\eta d\theta, \end{cases} \quad x \in (0, \delta). \tag{A2}$$

Equations (A1) and (A2) read as the solution (u, v) is a fixed point of the function Φ on $M_{a,b}$. This what we will prove indeed, using fixed point theory of contractive functions. We immediately get

$$|\Phi_1(u, v)(x) - a| \leq \frac{\delta^2}{2} C_1(p, q, \omega, a, b, c) \quad \text{and} \quad |\Phi_2(u, v)(x) - b| \leq \frac{\delta^2}{2} C_2(p, q, \omega, a, b, c), \tag{A3}$$

where

$$C_1(p, q, \omega, a, b, c) = c^p a^p + c^{2-q} b^{q-1} a + c\omega a \quad \text{and} \quad C_2(p, q, \omega, a, b, c) = a^{q-1} b + b^p + \omega b.$$

Choosing suitably δ, we may transform (A3) to

$$a \leq \Phi_1(u, v)(x) \leq ca \quad \text{and} \quad c^{-1}b \leq \Phi_2(u, v)(x) \leq b, \;\; x \in (0, \delta).$$

Hence, Φ is well-defined. We will show that it is contractive. Indeed, for (u_1, v_1) and (u_2, v_2) in $M_{a,b}$, we get

$$|f_\omega(u_1, v_1) - f_\omega(u_2, v_2)| \leq (pa^{p-1} + c^{1-q} b^{q-1} + \omega)|u_1 - u_2| + (1 - q)ac^{1-q} b^{q-2} |v_1 - v_2|. \tag{A4}$$

Similarly, we get

$$|f_\omega(v_1, u_1) - f_\omega(v_2, u_2)| \leq (1 - q)a^{q-2} b|u_1 - u_2| + (pb^{p-1} + a^{q-1} + \omega)|v_1 - v_2|. \tag{A5}$$

Denote also

$$K_0 = \max\Big(pa^{p-1} + c^{1-q} b^{q-1} + \;\omega, (1 - q)ac^{1-q} b^{q-2}, \; (1 - q)a^{q-2} b, \; a^{q-1} + \omega\Big). \tag{A6}$$

We obtain from (A4)–(A6),

$$\begin{cases} \|\Phi_1(u_1, v_1) - \Phi_1(u_2, v_2)\|_\infty \leq K_0 \dfrac{\delta^2}{2} \|(u_1 - u_2, v_1 - v_2)\|_\infty, \\ \|\Phi_2(u_1, v_1) - \Phi_2(u_2, v_2)\|_\infty \leq K_0 \dfrac{\delta^2}{2} \|(u_1 - u_2, v_1 - v_2)\|_\infty. \end{cases} \tag{A7}$$

Equation (A7) gives

$$\|\Phi(u_1, v_1) - \Phi(u_2, v_2)\|_\infty \leq K_0 \frac{\delta^2}{2} \|(u_1 - u_2, v_1 - v_2)\|_\infty.$$

So as the contractivity of Φ, which implies the exitence and uniqueness of the solution (u, v) on $(0, \delta)$.

To finish, we shall show that the solution (u, v) is global on $(0, \infty)$. Indeed, whenever the solution blows-up in some point $x_0 \in (0, \infty)$, we get a blowing-up energy $E(u, v)$ at x_0, which contradicts the constant aspect of this energy.

References

1. Benci, V.; Fortunato, D.F. *Variational Methods in Nonlinear Field Equations: Solitary Waves, Hylomorphic Solitons and Vortices*; Springer Monographs in Mathematics; Springer: Cham, Switzerland, 2014.
2. Benci, V.; Fortunato, D.F. Solitary waves of the nonlinear Klein-Gordon equation coupled with Maxwell equations. *Rev. Math. Phys.* **2020**, *14*, 409–420.
3. Ben Mabrouk, A.; Ayadi, M. A linearized finite-difference method for the solution of some mixed concave and convex nonlinear problems. *Appl. Math. Comput.* **2008**, *197*, 1–10.
4. Ben Mabrouk, A.; Ayadi, M. Lyapunov type operators for numerical solutions of PDEs. *Appl. Math. Comput.* **2008**, *204*, 395–407.
5. Ben Mabrouk, A.; Ben Mohamed, M.L.; Omrani, K. Finite difference approximate solutions for a mixed sub-superlinear equation. *Appl. Math. Comput.* **2007**, *187*, 1007–1016.
6. Ben Mabrouk, A.; Ben Mohamed, M.L. Nodal solutions for some nonlinear elliptic equations. *Appl. Math. Comput.* **2007**, *186*, 589–597.
7. Ben Mabrouk, A.; Ben Mohamed, M.L. Phase plane analysis and classification of solutions of a mixed sublinear-superlinear elliptic problem. *Nonlinear Anal. Theory Methods Appl.* **2009**, *70*, 1–15.
8. Ben Mabrouk, A.; Ben Mohamed, M.L. Nonradial solutions of a mixed concave-convex elliptic problem. *J. Partial Differ. Equ.* **2011**, *24*, 313–323.
9. Ben Mabrouk, A.; Ben Mohamed, M.L. On some critical and slightly super-critical sub-superlinear equations. *Far East J. Appl. Math.* **2006**, *23*, 73–90.
10. Chteoui, R.; Ben Mabrouk, A.; Cattani, C. Mixed Concave–Convex Sub-Superlinear Schrödinger Equation: Survey and Development of Some New Cases. In *Nonlinear Analysis and Global Optimization*; Springer: Cham, Switzerland, 2021; Volume 167.
11. Chaib, K. Necessary and sufficient conditions of existence for a system involving the p-Laplacian $(0 < p < N)$. *J. Differ. Equ.* **2003**, *189*, 513–525.
12. Hioe, F.T. Solitary waves for two and three coupled nonlinear Schrödinger equations. *Phys. Rev. E* **1998**, *58*, 6700.
13. Kanna, T.; Lakshmanan, M.; Dinda, P.T.; et al. Soliton collisions with shape change by intensity redistribution in mixed coupled nonlinear Schrödinger equations. *Phys. Rev. E* **2006**, *73*, 026604.
14. Zhang, H.Q.; Meng, X.H.; Xu, T.; et al. Interactions of bright solitons for the (2+1)-dimensional coupled nonlinear Schrödinger equations from optical fibres with symbolic computation. *Phys. Scr.* **2007**, *75*, 537–542.
15. Zhida, Y. Multi-soliton solutions of coupled nonlinear Schrödinger Equations. *Chin. Phys. Lett.* **1987**, *4*, 185–187.
16. Chteoui, R.; Aljohani, A.F.; Ben Mabrouk, A. Classification and simulation of chaotic behaviour of the solutions of a mixed nonlinear Schrodinger system. *Electron. Res. Arch.* **2021**, *29*, 2561–2597.
17. Chteoui, R.; Aljohani, A.F.; Ben Mabrouk, A. Lyapunov-Sylvester computational method for numerical solutions of a mixed cubic-superlinear Schrodinger system. *Eng. Comput.* **2022**, *38*, 1081–1094.
18. Chteoui, R.; Aljohani, A.F.; Ben Mabrouk, A. Synchronous Steady state solutions of a symmetric mixed cubic-superlinear Schrödinger system. *Symmetry* **2021**, *13*, 190.
19. Gupta, M.R.; Som, B.K.; Dasgupta, B. Coupled nonlinear Schrödinger equations for Langmuir and elecromagnetic waves and extension of their modulational instability domain. *J. Plasma Phys.* **1981**, *25*, 499–507.
20. Liu, M. Ground states of linearly coupled Schrödinger systems. *Electron. J. Differ. Equ.* **2017**, *2017*, 1–10.
21. Pinar, Z.; Deliktas, E. Solution behaviors in coupled Schrödinger equations with full-modulated nonlinearities. *AIP Conf. Proc.* **2017**, *1815*, 080019.
22. Ping, L.; Lou, S.Y. Coupled Nonlinear Schrödinger Equation: Symmetries and Exact Solutions. *Commun. Theor. Phys.* **2009**, *51*, 27–34.
23. Saanouni, T. A note on coupled focusing nonlinear Schrödinger equations. *Appl. Anal.* **2016**, *95*, 2063–2080.
24. Zhou, S.; Liang, X.; Cheng, X. Numerical solution to coupled nonlinear Schrödinger equations on unbounded domains. *Math. Comput. Simul.* **2010**, *80*, 2362–2373.